

1
2
3
4
5
6
7
8
9
10
11
12
13
14
15
16
17
18
19
20
21
22
23
24
25
26
27
28
29
30
31
32
33
34
35
36
37
38
39
40
41
42
43
44
45
46
47
48
49
50
51

The neonatal Fc receptor is a pan-echovirus receptor

Stefanie Morosky^{1,2}, Azia Evans^{1,2}, Kathryn Lemon^{3,4}, Sandra Schmus^{3,4}, Christopher J. Bakkenist^{3,4}, Carolyn B Coyne^{1,2,5*}

¹Department of Pediatrics, University of Pittsburgh School of Medicine, Pittsburgh, PA USA, ²Center for Microbial Pathogenesis, UPMC Children’s Hospital of Pittsburgh, Pittsburgh, PA USA, ³Department of Radiation Oncology, University of Pittsburgh School of Medicine, Pittsburgh, PA USA, ⁴Department of Pharmacology and Chemical Biology, University of Pittsburgh School of Medicine, Pittsburgh, PA USA, ⁵R. K. Mellon Institute for Pediatric Research, UPMC Children’s Hospital of Pittsburgh, Pittsburgh, PA USA

*Address correspondence:

Carolyn Coyne, PhD
9116 Rangos Research Center
Children’s Hospital of Pittsburgh of UPMC
One Children’s Hospital Way
4401 Penn Avenue
Pittsburgh, PA 15224
Phone (412) 692-7519
Email coynec2@pitt.edu; coynec3@upmc.edu

52 **Abstract**

53 Echoviruses are the main causative agents of aseptic meningitis worldwide and are particularly
54 devastating in the neonatal population, where they are associated with severe hepatitis,
55 neurological disease including meningitis and encephalitis, and even death. Here, we identify the
56 neonatal Fc receptor (FcRn) as a pan-echovirus receptor. We show that loss of expression of
57 FcRn or its binding partner beta 2 microglubulin (β 2M) renders human brain microvascular cells
58 resistant to infection by a panel of echoviruses at the stage of virus attachment and that a blocking
59 antibody to β 2M inhibit echovirus infection in cell lines and in primary human fetal intestinal
60 epithelial cells. We also show that expression of human, but not mouse, FcRn renders non-
61 permissive human and mouse cells sensitive to echovirus infection and that the extracellular
62 domain of human FcRn directly binds echoviral particles and neutralizes infection. Lastly, we
63 show that primary cells isolated from mice that express human FcRn are highly susceptible to
64 echovirus infection. Our findings thus identify FcRn as a pan-echovirus receptor, which may
65 explain the enhanced susceptibility of neonates to echovirus infections.

66
67 **Significance**
68

69 Echoviruses are associated with aseptic meningitis and induce severe disease, and even death,
70 in neonates and young infants. Here, we identify the neonatal Fc receptor (FcRn) as a pan-
71 echovirus receptor. FcRn is expressed on the surface of the human placenta, and throughout life
72 in intestinal enterocytes, liver hepatocytes, and in the microvascular endothelial cells that line the
73 blood-brain barrier. This pattern of expression is consistent with the organ sites targeted by
74 echoviruses in humans, with the primary entry site of infection in the intestinal tract and
75 subsequent infection of secondary tissues including the liver and brain. These findings provide
76 important insights into echovirus pathogenesis and may explain the enhanced susceptibility of
77 infants and neonates to echovirus-induced disease.

78 **Introduction**

79 Echoviruses are small (~30nm) single stranded RNA viruses belonging to the *Picornaviridae*
80 family. These viruses make up the largest subgroup of the Enterovirus genus and consist of
81 approximately 30 serotypes. Enteroviruses are the main causative agents of aseptic meningitis
82 worldwide, with echovirus 9 (E9) and echovirus 30 (E30) amongst the most commonly circulating
83 serotypes (1). The neonatal and infant populations are at greatest risk for developing severe
84 echovirus-induced disease and infection within the first few weeks of life can be fatal (2, 3).
85 Enteroviral infections are also devastating in Neonatal Intensive Care Units (NICUs), where they
86 account for 15-30% of NICU-associated nosocomial viral infections and result in death of the
87 neonate in as many as 25% of cases (4-7), the majority of which result from echovirus 11 (E11)
88 infections (8). In neonates, vertical transmission may occur at the time of delivery following a
89 maternal infection in the days or weeks prior to delivery (9). In addition, echovirus infections have
90 also been observed *in utero*, both at late and earlier stages of pregnancy, where they are
91 associated with fetal death (10-14).

92 Echoviruses are primarily transmitted through the fecal-oral route where they target the
93 gastrointestinal epithelium. In primary human fetal-derived enteroids, echoviruses exhibit a cell
94 type specificity of infection and preferentially infect enterocytes (15). The basis for this cell-type
95 specific tropism is unclear. Decay accelerating factor (DAF/CD55) functions as an attachment
96 factor for some echoviruses (16), but DAF expression does not sensitize non-permissive cells to
97 infection (17), suggesting that another cell surface molecule functions as the primary receptor.
98 While integrin VLA-2 ($\alpha_2\beta_1$) is a primary receptor for E1 (18), it does not serve as a receptor for
99 other echoviruses. Other work has implicated a role for MHC class I receptors in echovirus
100 infections due to inhibition of viral binding, entry, or infection by monoclonal antibodies to MHC
101 class I and/or beta-2 microglobulin (β_2M) (17, 19, 20), which is required for efficient cell surface

102 trafficking of MHC class I receptors. However, the precise role for MHC class I and β 2M remains
103 unclear and the primary receptor for many echoviruses is unknown.

104 Here, we identify the human neonatal Fc receptor (FcRn) as a primary echovirus receptor.
105 We show that human cells deficient in FcRn expression are resistant to echovirus infection and
106 infection is restored by FcRn expression. Concomitantly, expression of human FcRn renders
107 murine-derived cell lines and primary cells permissive to echovirus infection. In contrast,
108 expression of the murine homolog of FcRn has no effect on viral infection in either human or
109 mouse cells, identifying a species-specific role for FcRn in echovirus infection. Using primary
110 human intestinal epithelial cell monolayers isolated from mid-gestation fetal small intestines, we
111 show that a monoclonal antibody recognizing β 2M, which non-covalently associates with FcRn
112 and is required for FcRn cell surface expression (21), significantly reduces echovirus infection.
113 Lastly, we show that recombinant FcRn in complex with β 2M neutralizes echovirus infection and
114 directly interacts with viral particles. Our data thus identify FcRn as a primary receptor for
115 echoviruses, which has important implications for echovirus pathogenesis.

116

117 **Results**

118 **Human cells deficient in FcRn are non-permissive to echovirus infection**

119 We screened a panel of cell lines for their susceptibility to echovirus infection and found that
120 human placental choriocarcinoma JEG-3 cells were resistant to infection by a panel of 7
121 echoviruses (E5-7, E9, E11, E13, and E30) but were highly permissive to the related enterovirus
122 coxsackievirus B3 (CVB) (**Figure 1A**). Levels of echovirus infection in JEG-3 cells were
123 comparable to those observed in mouse embryonic fibroblasts (MEFs), which are highly resistant
124 to echovirus infection, and were significantly less than those observed in permissive cell types
125 including human intestinal Caco-2, HeLa, human brain microvascular endothelial cells (HBMEC),
126 and human osteosarcoma U2OS cells (**Figure 1A, Supplemental Figure 1A-C**). The resistance

127 of JEG-3 cells to echovirus infection occurred at the level of viral binding or entry as infection was
128 restored when cells were transfected with infectious viral RNA (vRNA) (**Supplemental Figure**
129 **1D**).

130 We next performed RNAseq-based transcriptomics analyses between non-permissive
131 JEG-3 cells and permissive cell types including Caco-2 and HBMEC cells and primary human
132 enteroids harvested from fetal small intestines, which are highly sensitive to echovirus infection
133 (15), to identify cell surface receptors differentially downregulated in JEG-3 cells. Because JEG-
134 3 cells arise from choriocarcinomas and express many placental-specific transcripts, we also
135 included JAR cells in our analyses, another human choriocarcinoma line that is more permissive
136 to echovirus infection than JEG-3 cells (**Supplemental Figure 1E**). Using this approach, we
137 identified 118 transcripts differentially downregulated in JEG-3 cells ($p < 0.001$, \log_2 z score < -2 ,
138 **Figures 1B, 1C and Supplemental Table 1**). Of these 118 transcripts, the neonatal Fc receptor
139 (FCGRT, hereafter referred to as FcRn), was the most significantly downregulated cell surface
140 receptor in JEG-3 cells ($p < 0.001$, \log_2 z-score < -2), (**Figure 1D, Supplemental Table 1,**
141 **Supplemental Figure 1F**). We confirmed the significantly lower levels of expression of FcRn in
142 JEG-3 cells relative to permissive cell lines (HBMEC, HeLa, and JAR) and primary human fetal
143 enteroids using RT-qPCR (**Figure 1D**). In contrast, there were no differences in expression of
144 $\beta 2M$, which is required to traffic FcRn to the cell surface (21) (**Figure 1E**). In addition, we
145 confirmed previous findings that JAR cells are deficient in MHC class I molecules and that JEG-
146 3 cells express very low levels of MHC class I molecules (22) (**Supplemental Figure 1G**),
147 supporting the notion that these molecules were not responsible for the differential susceptibility
148 of JEG-3 cells to echovirus infections.

149 To determine if the lack of FcRn expression was directly responsible for the low levels of
150 echovirus infection in JEG-3 cells, we ectopically expressed human FcRn (hFcRn). Expression of
151 hFcRn in JEG-3 cells significantly increased their susceptibility to infection by E5, E11, and E30
152 (~10,000-fold, **Figure 1F, Supplemental Figure 1H**). In contrast, expression of the related MHC

153 class I or MHC class I-like molecules HLA-A and HLA-C and hemochromatosis protein (HFE),
154 which also require β 2M for cell surface expression, also had no effect on infection (**Figure 1F**,
155 **Supplemental Figure H-I**). These data show that expression of hFcRn restores echovirus
156 infection in non-permissive human cells.

157

158 **Expression of human FcRn restores echovirus infection in mouse cells**

159 Echoviruses do not infect mouse cells efficiently (**Supplemental Figure 1A, 1B**). Since ectopic
160 expression of hFcRn in human cells in which endogenous levels were low restored their
161 susceptibility to infection, we next determined whether the murine homolog of FcRn (mFcRn) was
162 also sufficient to promote infection. Whereas expression of hFcRn in JEG-3 cells restored
163 infection of a panel of echoviruses (E5, E7, E11, E13, and E30) by \sim 10,000-fold, expression of
164 mFcRn had no significant effect (**Figure 2A, Supplemental Figure 2A, 2B**). Similarly, we found
165 that expression of hFcRn, but not mFcRn, rendered mouse embryonic fibroblasts (MEFs) and
166 chinese hamster ovary (CHO) cells highly susceptible to echovirus infection (**Figure 2B**,
167 **Supplemental Figure 2D**).

168 To further define the role of hFcRn in echovirus infection, we isolated primary fibroblasts
169 from mice lacking expression of mFcRn, but expressing the α chain of hFcRn under the control
170 of the endogenous promoter (mFcRn^{-/-} hFcRn^{+/+}) or matched wild-type controls (mFcRn^{+/+} hFcRn⁻
171 ^{-/-}) (**Figure 2C**) (23, 24). In these cells, hFcRn is expressed at the cell surface in complex with
172 mouse β 2M. Primary fibroblasts isolated from mFcRn^{+/+} hFcRn^{-/-} mice were resistant to echovirus
173 infection, as expected (**Figure 2D, 2E**). In contrast, cells isolated from mFcRn^{-/-} hFcRn^{+/+} mice
174 were highly permissive to echovirus infection and exhibited $>$ 10,000-fold enhanced susceptibility
175 to infection (**Figure 2D, 2E**). Collectively, these data show that expression of human, but not
176 mouse FcRn is sufficient to confer cellular susceptibility to echovirus infection, which supports a
177 species-specific role for FcRn in echovirus infections.

178

179 **Loss of FcRn expression renders cells resistant to echovirus infection**

180 We next determined whether loss of FcRn expression rendered cells expressing FcRn less
181 susceptible to infection. For these studies, we used RNAi-mediated silencing of FcRn in HBMEC,
182 an immortalized human blood-brain barrier cell line that expresses high levels of FcRn (**Figure**
183 **1C, 1D**) and which is highly sensitive to echovirus infection (**Supplemental Figure 1A, 1B**). We
184 found that silencing of FcRn expression by two independent siRNAs led to significant (~1000-
185 10,000-fold) decreases in echovirus infection but had no effect on CVB infection (**Figure 3A, 3B,**
186 **Supplemental Figure 3A**). Similar results were obtained in human osteosarcoma U2OS cells
187 (**Supplemental Figure 3B**). In addition, silencing of β 2M expression led to comparable reductions
188 in infection (**Figure 3A-B, Supplemental Figure 3A-C**). In contrast, RNAi-mediated silencing of
189 other cell surface molecules that require β 2M for trafficking, such as HLA-A, HLA-B, HLA-C, and
190 HFE had no significant effect on echovirus infection in HBMEC (**Supplemental Figure 3C**).
191 Importantly, echovirus replication in β 2M- and hFcRn-RNAi transfected cells was restored when
192 cells were transfected with infectious vRNA (**Figure 3C**), suggesting that the inhibition occurred
193 at the stage of virus binding or entry.

194 To determine whether other echoviruses also required expression of FcRn, we performed
195 a high content imaging-based screen using β 2M siRNA and two siRNAs targeting FcRn (alone
196 and in combination) for a panel of echoviruses (E5, E6-7, E9, E11, E13, E25, E29, and E30-32)
197 as well as CVB as a control. We found that infection by all echoviruses tested was significantly
198 reduced in cells depleted of β 2M or FcRn expression while CVB infection was unchanged
199 (**Supplemental Figure 3E**). In addition, consistent with previous studies that blocking antibodies
200 to β 2M inhibited infection of E7 and E11 (17, 19), we found that infection by E5, E7, E9, E11, E13,
201 and E30 were also inhibited by a monoclonal antibody against β 2M (**Supplemental Figure 3F**).

202 Because echoviruses are transmitted by the enteral route and infect the gastrointestinal
203 epithelium as the primary site of host entry, we next determined whether FcRn was also involved
204 in echovirus infection of intestinal epithelial cells. We showed previously that E11 preferentially
205 infects enterocytes in human fetal-derived enteroids (15). To determine the role of FcRn in
206 echovirus infection of the human neonatal intestine, we isolated intestinal crypts from human fetal
207 small intestines (16-23w of gestation) and plated these crypts directly onto transwell inserts which
208 leads to the formation of a fully differentiated single cell monolayer. We found that FcRn localized
209 to the sub-apical domain of fetal-derived primary human intestinal epithelial (HIE) monolayers
210 (**Figure 3D, left**), which is consistent with what has been observed *in vivo* in other polarized cells
211 types, where FcRn localizes sub-apically and to the basolateral surface (25-29) whereas β 2M
212 was localized to both the basolateral contact sites and to intracellular vesicles (**Figure 3D, right**).
213 Because primary HIE cannot be genetically altered, we used β 2M monoclonal antibody to
214 determine whether FcRn also facilitates echovirus infection of these cells. In HIE collected from
215 three different human fetal intestine preparations, we found that β 2M monoclonal antibody
216 significantly reduced infection by E7, E11, and E30 (**Figure 3E**), similar to that which we observed
217 in cell lines. Collectively, these data show that FcRn expression is required for echovirus infection
218 and implicates a role for FcRn in mediating echovirus infection of the human neonatal intestine.

219

220 **FcRn facilitates echovirus attachment and directly interacts with viral particles**

221 We found that echovirus infection in cells depleted of FcRn could be restored by transfection of
222 cells with vRNA, which suggested that this inhibition occurred at the stage of viral binding or entry.
223 We therefore determined whether downregulation of FcRn expression would alter echovirus
224 binding. We found that silencing of FcRn expression in HBMEC significantly reduced cell surface
225 binding of E5, E7, E9, E11, and E30 to HBMEC (**Figure 4A**). In contrast, this silencing had no
226 effect on CVB binding (**Figure 4A**). Residual levels of viral binding in HBMEC may be mediated

227 by cell surface factors such as DAF that facilitate binding of some echoviruses (16). Consistent
228 with a role in viral binding, we also found that echovirus binding to primary mouse fibroblasts
229 (mFcRn^{-/-}, hFcRn^{+/+}) was significantly higher than in cells expressing mFcRn (mFcRn^{+/+}, hFcRn^{-/-}
230) (**Figure 4B**). These data show that FcRn facilitates echovirus cell surface attachment.

231 To determine whether FcRn directly interacts with echovirus particles, we used a
232 recombinant protein approach utilizing a purified heterodimer containing the extracellular domain
233 of FcRn in complex with β 2M (rFcRn- β 2M). We found that incubation of viral particles with rFcRn-
234 β 2M prior to infection neutralized both E11 and E30 infection (**Figure 4C, 4D**). In contrast,
235 incubation with purified β 2M alone, or recombinant HLA-A or HLA-C had no effect (**Figure 4C,**
236 **4D**). To determine whether there was a direct interaction between FcRn and echoviral particles,
237 we performed *in vitro* binding assays using rFcRn- β 2M. Using this approach, we found that rFcRn-
238 β 2M co-precipitated with purified E11 and E30 in *in vitro* binding assays, (**Figure 4E**),
239 demonstrating a direct interaction between FcRn and echovirus particles.

240

241 Discussion

242 Here, we identify FcRn as a primary receptor for echoviruses. We show that expression
243 of FcRn is necessary and sufficient for echovirus infection and that FcRn directly binds echovirus
244 particles and facilitates viral binding. We also show that expression of human, but not mouse
245 FcRn restores echovirus infection in non-permissive mouse and human cells and thereby identify
246 a species-specific mechanism of infection. Our data show that a number of clinically relevant
247 echoviruses commonly associated with human disease, including E9, E30, and E11, utilize FcRn
248 as a receptor, suggesting a pan-echovirus role. In contrast, FcRn plays no role in the infection of
249 related enteroviruses including CVB and PV. Our findings provide important insights into the
250 cellular receptor used by echoviruses to initiate their infections, which also provides further
251 insights into a variety of aspects of echovirus pathogenesis.

252 FcRn transports and regulates the circulating half-life of IgG throughout life (30-32). In
253 addition, FcRn is responsible for the development of passive immunity through the transfer of
254 maternal-derived antibodies. In humans, expression of FcRn on the placenta (33) is solely
255 responsible for the establishment of passive immunity in the fetus due to transport of maternal-
256 derived IgG across the placental surface directly into fetal blood (34). This differs in rodents, where
257 passive immunity is established postnatally from maternal-derived IgG in milk/colostrum (35).
258 FcRn is expressed throughout life in a variety of cell types including the small intestine (26, 36),
259 the microvasculature of the blood-brain barrier (37), myeloid cells (38), hepatocytes (39, 40),
260 amongst others. Although echoviruses are primarily transmitted via the fecal-oral route, viral-
261 induced disease is associated with infection of secondary organs, most notably the liver and brain.
262 The expression of FcRn on the surfaces of the intestine, brain microvasculature, and hepatocytes
263 may thus explain the tropism of echoviruses for these tissues and the viral mechanism to bypass
264 the barriers presented by the cells comprising these sites.

265 FcRn binds albumin as well as IgG (39, 41). Although FcRn binds to albumin and IgG at
266 distinct sites (42), both of these interactions occur within the low pH (≤ 6.5) environment of
267 endosomes, with release occurring in the basic pH (≤ 7.5) of the bloodstream. In contrast, our
268 findings reveal a direct interaction between echoviruses and FcRn that occurs at the neutral pH
269 of the cell surface prior to viral entry. Once internalized, it is possible that the interaction between
270 FcRn and echoviruses is altered by the low pH of endosomes, which may facilitate subsequent
271 genome release and/or endosomal escape. We have shown that E11 preferentially infects
272 enterocytes (15), with enhanced infection from the basolateral surface of HIE (43). This polarity
273 of infection is consistent with the enhanced expression of FcRn in enterocytes in the intestine and
274 its enrichment to the basolateral surface. Following replication, E11 is released bidirectionally
275 from HIE from both the apical and basolateral domains (43). Given that FcRn mediates

276 bidirectional transport (29), this raises the possibility that echoviruses could be transported from
277 either the apical or basolateral domains to cross the intestinal barrier.

278 Echoviruses are associated with severe disease in neonates, particularly during the first
279 two weeks of life and in those born prematurely. The vertical transmission of echoviruses is
280 thought to occur at the time of delivery and be associated with maternal infection in the preceding
281 days or weeks. However, fetal infections *in utero* have also been associated with disease and/or
282 death (10-14), suggesting that vertical transmission might also occur during pregnancy. FcRn is
283 highly expressed on syncytiotrophoblasts (30, 44), the fetal-derived cells that comprise the
284 outermost cellular barrier of the human placenta that directly contact maternal blood. These cells
285 are highly resistant to viral infections due to intrinsic antiviral defense pathways (33). However,
286 given that FcRn expressed on the surface of these cells transcytoses maternal-derived IgG
287 directly into the underlying fetal blood. Our identification of FcRn as an echovirus receptor raises
288 the possibility that echoviruses might have higher rates of transplacental transfer than has been
289 appreciated. In addition, it should be noted that the highest rates of transplacental IgG transfer
290 occur in the third trimester, with the level of maternal-derived IgG is greater in the fetus than in
291 the mother (45). Thus, a maternal echovirus infection in the later stages of pregnancy could
292 potentially lead to FcRn-mediated placental infection or transplacental viral transport and expose
293 the fetus to virus prior to delivery. Further defining the role of FcRn in echovirus infections *in utero*
294 and postnatally will provide important insights into echovirus-induced fetal and neonatal disease.

295 Our work presented here identifies FcRn as a pan-echovirus receptor. Given that FcRn-
296 based therapeutics have been developed to target a variety of human diseases (46), our findings
297 also point to FcRn as a possible target for anti-echovirus therapeutics to ameliorate virus-induced
298 disease. Future studies identifying the mechanism by which echoviruses utilize FcRn to enter or
299 bypass barrier tissues such as the GI epithelium, blood-brain barrier, and placenta will provide
300 important insights into a variety of aspects of echovirus pathogenesis.

301

302 **Materials and Methods**

303 *Additional Materials and Methods are located in Supplemental Information*

304 **Cell lines**

305 Human brain microvascular cells (HBMEC) were obtained from Kwang Sik Kim (Johns Hopkins
306 University) and have been described previously (47) and were grown in RPMI-1640
307 supplemented with 10% fetal bovine serum (FBS, Invitrogen), 10% NuSerum (Corning), non-
308 essential amino acids (Invitrogen), sodium pyruvate, MEM vitamin solution (Invitrogen), and
309 penicillin/streptomycin. JEG-3, JAR, U2OS, and Caco-2 (BBE clone) cells were purchased from
310 the ATCC and were cultured as described previously (48, 49). HeLa cells (clone 7B) were
311 provided by Jeffrey Bergelson (Children's Hospital of Philadelphia) and were cultured in MEM
312 supplemented with 5% FBS and penicillin/streptomycin.

313

314 **Primary cells**

315 Experimental procedures were approved by the University of Pittsburgh Animal Care and Use
316 Committee and all methods were performed in accordance with the relevant guidelines and
317 regulations. Primary fibroblasts were generated from 4 week old B6.Cg-Fcgrt^{tm1Dcr} Tg(CAG-
318 FCGRT) 276Dcr/DcrJ (Cat. 004919) and control C57BL/6J (000664) mice purchased from The
319 Jackson Laboratory (Bar Harbor, Maine). Mice were euthanized according to institution standards
320 and ears and tail were removed, incubated in 70% ethanol for 5min and then rinsed twice in PBS
321 + 50ug/mL kanamycin for 5 min. Hair was removed and tissue was cut into small pieces and
322 incubated in 9.4mg/mL collagenase D (Roche, 11088858001) and 1.2 mg/mL pronase (Roche,
323 1088858001) in complete DMEM at 37°C with shaking at 200rpm for 90min. The resulting cell
324 suspensions were filtered through 70uM cell strainers, collected at 580g, resuspended in
325 complete DMEM containing 10 units penicillin and 10ug streptomycin/mL and 250ng/mL
326 amphotericin B and cultured at 37°C in a humidified 5% CO₂ incubator.

327 Primary human intestinal epithelial cells were isolated from crypts isolated from human
328 fetal small intestines as described (15). Complete methods can be found in Supplemental
329 Materials and Methods.

330

331 **Viruses and viral infections**

332 Experiments were performed with coxsackievirus B3 (CVB) RD strain, poliovirus (PV, sabin strain,
333 type 2), echovirus 5 (Noyce stain, E5), echovirus 6 (Burgess strain, E6), echovirus 7 (Wallace
334 strain, E7), echovirus 9 (Hill strain, E9), echovirus 11 (Gregory or Silva strains, E11^G and E11^S),
335 echovirus 13 (Del Carmen, E13), echovirus 25 (JV-4, E25), echovirus 29 (JV-10, E29), echovirus
336 30 (Bastianni strain, E30), echovirus 31 (Caldwell strain, E31), or echovirus 32 (PR-10 strain,
337 E32) that were provided by Jeffrey Bergelson (Children's Hospital of Philadelphia) and were
338 originally obtained from the ATCC. Viruses were propagated in HeLa cells and purified by
339 ultracentrifugation over a sucrose cushion, as described (50).

340 Unless otherwise stated, infections were performed with 1 PFU/cell of the indicated virus.
341 In some cases, viruses were pre-adsorbed to cells for 1hr at 4°C in serum-free MEM
342 supplemented with 10mM HEPES followed by extensive washing in 1x PBS or complete media.
343 Infections were then initiated by shifting cells to 37°C for the times indicated. Viral titers were
344 determined by TCID₅₀ assays in HeLa cells using crystal violet staining.

345 Binding assays were performed by pre-adsorbing 50 PFU/cell of the indicated virus to
346 cells for 1hr at 4°C in serum-free MEM supplemented with 10mM HEPES followed by extensive
347 washing with 1x PBS. Immediately following washing, RNA was isolated, and RT-qPCR
348 performed for viral genome-specific primers, as described below.

349 For experiments using blocking antibodies, cells were incubated with the indicated
350 antibodies (at 5µg/mL) for 1hr at 4°C in serum-free DMEM containing 10mM HEPES. For anti-
351 DAF IF7 blocking experiments, all incubations were performed in DMEM containing 10% FBS
352 and 10mM HEPES. Following this incubation, viruses were pre-adsorbed to cells in the presence

353 of antibodies for an additional 1hr at 4oC in serum-free or serum-containing medium, washed
354 extensively, and then cells infected at 37oC for the indicated time in the presence of

355

356 **Plasmids, siRNAs, and transfections**

357 Sequence verified vectors (pcDNA 3.1) expressing human HLA-A (, HLA-C, FcRn or mouse FcRn
358 were purchased from Genscript. EGFP-fused HFE (pCB6-HFE-EGFP) was a gift from Pamela
359 Bjorkman (Addgene plasmid # 12104) and was described previously (51). Plasmids were reverse
360 (MEFs, CHO cells) or forward (JEG-3 cells) transfected with the indicated plasmids using
361 Lipofectamine 3000 according to the manufacturer's instructions.

362 Pooled siRNAs (four total) targeting HLA-A and HFE were purchased from Dharmacon
363 (siGENOME, M-012850-01 and M-011051-02). Pooled siRNAs (four total) targeting HLA-B and
364 HLA-C were purchased from Santa Cruz Biotechnology (sc-42922 and sc-105525). Control
365 (scrambled) siRNA was purchased from Sigma (Mission Universal, SIC001). Individual siRNAs
366 targeting were synthesized by Sigma, with sequences as follows: (β 2M
367 UCCAUCCGACAUUGAAGUU; FcRn-1 CCACAGAUCUGAGGAUCAA; FcRn-2
368 ACUUUUGACUGUUAGUGAC). In all cell types, siRNAs were reverse transfected into cells using
369 Dharmafect-1 (Dharmacon) according to the manufacturer's instructions.

370

371 **Antibodies**

372 The following antibodies or reagents were used—recombinant anti-dsRNA antibody (provided by
373 Abraham Brass, University of Massachusetts and described previously (52)), mouse monoclonal
374 anti-VP1 (NCL-ENTERO, Leica), mouse monoclonal anti-FcRn (Santa Cruz Biotechnology, sc-
375 271745), rabbit polyclonal FcRn (Abcam ab139152), rabbit monoclonal HLA-A (Abcam,
376 ab52922), rabbit monoclonal HLA-C (Abcam, ab126722), PE-conjugated anti-HLA antibody
377 (recognizing HLA A-C, HLA-E) (Novus, NBP2-68006PE), mouse monoclonal anti- β 2M (Sigma,

378 SAB4700010), and isotype control mouse monoclonal IgG antibody (MOPC 21, Sigma, M5284).
379 Alexa-fluor 594 conjugated phalloidin was purchased from Invitrogen (A12381). Anti-DAF IF7
380 antibody was provided by Jeffrey Bergelson (Children's Hospital of Philadelphia).

381

382 **Recombinant protein, *in vitro* pulldowns, and immunoblotting**

383 Purified native β 2M was purchased from Bio-rad (6240-0824) and was isolated from human urine.
384 Recombinant HLA-A and HLA-C was purchased from Novus (H00003105 and NBP2-2310,
385 respectively). Recombinant extracellular domain of FcRn in complex with β 2M was purchased
386 from Sino Biological (CT009-H08H) and was purified from HEK293 cells. For viral neutralization
387 studies, purified viral particles (10^6) were incubated with the indicated recombinant protein ($2\mu\text{g}$)
388 for 1hr at 4°C with constant rotation in serum-free MEM supplemented with 10mM HEPES. This
389 complex was then added to cells for an additional 1hr at 4°C , cells washed extensively with 1x
390 PBS, and infections initiated by shifting to 37°C for the 16-24hrs, as indicated in figure legends.

391 *In vitro* pulldowns between E11 and E30 were performed by incubating purified virus
392 particles (10^7) with $2\mu\text{g}$ of purified 6xHis tagged FcRn complex to β 2M for 1hr at 4°C with constant
393 rotation in buffer containing 100mM NaCl, 20mM Tris-Cl (pH 7.4), 0.5mM EDTA, and 0.5% (v/v
394 Nonidet-40). Following this incubation, HiPur Ni-NTA agarose beads were added for an additional
395 1hr at 4°C with constant rotation. Bead complexes were then pelleted by centrifugation and
396 washed 6x with wash buffer (10mM Tris-Cl (pH 8.0), 1mM EDTA, 1% Triton X-100, 0.1% SDS,
397 and 140mM NaCl). Beads were then resuspended in denaturing sample buffer and immunoblots
398 performed, as described below.

399 For immunoblotting, the lysates described above were loaded onto 4-20% Tris-HCl gels
400 (Bio-Rad) and transferred to nitrocellulose membranes. Membranes were blocked in 5% nonfat
401 dry milk, probed with the indicated antibodies, and developed with horseradish peroxidase-
402 conjugated secondary antibodies (Santa Cruz Biotechnology), and SuperSignal West Dura

403 chemiluminescent substrates (Pierce Biotechnology). Membranes were stripped for reprobing
404 using ReBlot Strong antibody stripping solution (Millipore, 2504) according to the manufacturer's
405 instructions.

406

407 **Immunofluorescence microscopy**

408 Cells were washed with PBS and fixed with ice-cold 100% methanol for immunostaining of viral
409 infections or with 4% paraformaldehyde at room temperature, followed by 0.25% Triton X-100 to
410 permeabilize cell membranes for a minimum of 15min at room temperature for all other
411 immunostaining. Cells were incubated with primary antibodies for 1 hour at room temperature,
412 washed with 1x PBS, and then incubated for 30 minutes at room temperature with Alexa-Fluor-
413 conjugated secondary antibodies (Invitrogen). Slides were washed and mounted with Vectashield
414 (Vector Laboratories) containing 4',6-diamidino-2-phenylindole (DAPI). Images were captured
415 using a Zeiss LSM 710 inverted laser scanning confocal microscope or with inverted IX81 or IX83
416 Olympus fluorescent microscopes. Images were adjusted for brightness/contrast using Adobe
417 Photoshop (Adobe). Image quantification for the extent of infection was performed using Fiji (Cell
418 counter plugin) or the CellSens Count and Measure package, as indicated. A minimum of 1000
419 cells were quantified.

420

421 **RT-qPCR**

422 Total RNA was prepared using the Sigma GenElute total mammalian RNA miniprep kit, according
423 to the protocol of the manufacturer. RNA was reverse transcribed with the iScript cDNA synthesis
424 kit (Bio-Rad) following the manufacturer's instructions. A total of 1 µg of total RNA was reversed
425 transcribed in a 20 µL reaction, and subsequently diluted to 100 µL for use. RT-qPCR was
426 performed using the iQ SYBR Green Supermix or iTaq Universal SYBR Green Supermix (Bio-
427 Rad) on a CFX96 Touch Real-Time PCR Detection System (Bio-Rad). Gene expression was
428 determined based on a ΔC_Q method, normalized to human actin. Primer sequences to actin, CVB,

429 and pan-echovirus primers have been described previously (49, 53). Primers to β 2M, FcRn, HLA-
430 A, HLA-B, HLA-C, and HFE were synthesized by Sigma and sequences can be found in
431 Supplemental Table 2.

432

433 **Statistics**

434 All statistical analysis was performed using GraphPad Prism. Experiments were performed at
435 least three times. Data are presented as mean \pm standard deviation. A Student's t-test or One-
436 Way Anova was used to determine statistical significance, as described in figure legends. P
437 values of < 0.05 were considered statistically significant, with specific P-values noted in the figure
438 legends.

439

440

441

442

443

444

445

446

447

448

449

450

451

452

453

454

455 **Literature cited**

- 456 1. Centers for Disease C & Prevention (2006) Enterovirus surveillance--United States,
457 2002-2004. *MMWR Morb Mortal Wkly Rep* 55(6):153-156.
- 458 2. Haston JC & Dixon TC (2015) Nonpolio enterovirus infections in neonates. *Pediatr Ann*
459 44(5):e103-107.
- 460 3. Tebruegge M & Curtis N (2009) Enterovirus infections in neonates. *Semin Fetal*
461 *Neonatal Med* 14(4):222-227.
- 462 4. Civardi E, *et al.* (2013) Viral outbreaks in neonatal intensive care units: what we do not
463 know. *Am J Infect Control* 41(10):854-856.
- 464 5. Naing Z, *et al.* (2013) Prevalence of viruses in stool of premature neonates at a neonatal
465 intensive care unit. *J Paediatr Child Health* 49(3):E221-226.
- 466 6. Verboon-Maciolek MA, Krediet TG, Gerards LJ, Fler A, & van Loon TM (2005) Clinical
467 and epidemiologic characteristics of viral infections in a neonatal intensive care unit
468 during a 12-year period. *Pediatr Infect Dis J* 24(10):901-904.
- 469 7. Isaacs D, *et al.* (1989) Conservative management of an echovirus 11 outbreak in a
470 neonatal unit. *Lancet* 1(8637):543-545.
- 471 8. Khetsuriani N, Lamonte A, Oberste MS, & Pallansch M (2006) Neonatal enterovirus
472 infections reported to the national enterovirus surveillance system in the United States,
473 1983-2003. *Pediatr Infect Dis J* 25(10):889-893.
- 474 9. Pedrosa C, Lage MJ, & Virella D (2013) Congenital echovirus 21 infection causing
475 fulminant hepatitis in a neonate. *BMJ Case Rep* 2013.
- 476 10. Tassin M, *et al.* (2014) A case of congenital Echovirus 11 infection acquired early in
477 pregnancy. *J Clin Virol* 59(1):71-73.
- 478 11. Viskari HR, *et al.* (2002) Maternal first-trimester enterovirus infection and future risk of
479 type 1 diabetes in the exposed fetus. *Diabetes* 51(8):2568-2571.
- 480 12. Garcia AG, Basso NG, Fonseca ME, & Outani HN (1990) Congenital echo virus
481 infection--morphological and virological study of fetal and placental tissue. *J Pathol*
482 160(2):123-127.
- 483 13. Basso NG, *et al.* (1990) Enterovirus isolation from foetal and placental tissues. *Acta Virol*
484 34(1):49-57.
- 485 14. Nielsen JL, Berryman GK, & Hankins GD (1988) Intrauterine fetal death and the isolation
486 of echovirus 27 from amniotic fluid. *J Infect Dis* 158(2):501-502.
- 487 15. Drummond CG, *et al.* (2017) Enteroviruses infect human enteroids and induce antiviral
488 signaling in a cell lineage-specific manner. *Proc Natl Acad Sci U S A* 114(7):1672-1677.

- 489 16. Bergelson JM, *et al.* (1994) Decay-accelerating factor (CD55), a
490 glycosylphosphatidylinositol-anchored complement regulatory protein, is a receptor for
491 several echoviruses. *Proc Natl Acad Sci U S A* 91(13):6245-6248.
- 492 17. Chevaliez S, *et al.* (2008) Role of class I human leukocyte antigen molecules in early
493 steps of echovirus infection of rhabdomyosarcoma cells. *Virology* 381(2):203-214.
- 494 18. Bergelson JM, Shepley MP, Chan BM, Hemler ME, & Finberg RW (1992) Identification
495 of the integrin VLA-2 as a receptor for echovirus 1. *Science* 255(5052):1718-1720.
- 496 19. Ward T, *et al.* (1998) Role for beta2-microglobulin in echovirus infection of
497 rhabdomyosarcoma cells. *J Virol* 72(7):5360-5365.
- 498 20. Goodfellow IG, *et al.* (2000) Echovirus infection of rhabdomyosarcoma cells is inhibited
499 by antiserum to the complement control protein CD59. *J Gen Virol* 81(Pt 5):1393-1401.
- 500 21. Praetor A & Hunziker W (2002) beta(2)-Microglobulin is important for cell surface
501 expression and pH-dependent IgG binding of human FcRn. *J Cell Sci* 115(Pt 11):2389-
502 2397.
- 503 22. Apps R, *et al.* (2009) Human leucocyte antigen (HLA) expression of primary trophoblast
504 cells and placental cell lines, determined using single antigen beads to characterize
505 allotype specificities of anti-HLA antibodies. *Immunology* 127(1):26-39.
- 506 23. Petkova SB, *et al.* (2006) Enhanced half-life of genetically engineered human IgG1
507 antibodies in a humanized FcRn mouse model: potential application in humorally
508 mediated autoimmune disease. *Int Immunol* 18(12):1759-1769.
- 509 24. Roopenian DC, Christianson GJ, & Sproule TJ (2010) Human FcRn transgenic mice for
510 pharmacokinetic evaluation of therapeutic antibodies. *Methods Mol Biol* 602:93-104.
- 511 25. Praetor A, Ellinger I, & Hunziker W (1999) Intracellular traffic of the MHC class I-like IgG
512 Fc receptor, FcRn, expressed in epithelial MDCK cells. *J Cell Sci* 112 (Pt 14):2291-
513 2299.
- 514 26. Shah U, *et al.* (2003) Distribution of the IgG Fc receptor, FcRn, in the human fetal
515 intestine. *Pediatr Res* 53(2):295-301.
- 516 27. Claypool SM, *et al.* (2004) Bidirectional transepithelial IgG transport by a strongly
517 polarized basolateral membrane Fc gamma-receptor. *Mol Biol Cell* 15(4):1746-1759.
- 518 28. McCarthy KM, Yoong Y, & Simister NE (2000) Bidirectional transcytosis of IgG by the rat
519 neonatal Fc receptor expressed in a rat kidney cell line: a system to study protein
520 transport across epithelia. *J Cell Sci* 113 (Pt 7):1277-1285.
- 521 29. Dickinson BL, *et al.* (1999) Bidirectional FcRn-dependent IgG transport in a polarized
522 human intestinal epithelial cell line. *J Clin Invest* 104(7):903-911.
- 523 30. Simister NE & Mostov KE (1989) An Fc receptor structurally related to MHC class I
524 antigens. *Nature* 337(6203):184-187.

- 525 31. Junghans RP & Anderson CL (1996) The protection receptor for IgG catabolism is the
526 beta2-microglobulin-containing neonatal intestinal transport receptor. *Proc Natl Acad Sci*
527 *U S A* 93(11):5512-5516.
- 528 32. Israel EJ, Patel VK, Taylor SF, Marshak-Rothstein A, & Simister NE (1995) Requirement
529 for a beta 2-microglobulin-associated Fc receptor for acquisition of maternal IgG by fetal
530 and neonatal mice. *J Immunol* 154(12):6246-6251.
- 531 33. Arora N, Sadovsky Y, Dermody TS, & Coyne CB (2017) Microbial Vertical Transmission
532 during Human Pregnancy. *Cell Host Microbe* 21(5):561-567.
- 533 34. Roopenian DC & Akilesh S (2007) FcRn: the neonatal Fc receptor comes of age. *Nat*
534 *Rev Immunol* 7(9):715-725.
- 535 35. Jones EA & Waldmann TA (1972) The mechanism of intestinal uptake and transcellular
536 transport of IgG in the neonatal rat. *J Clin Invest* 51(11):2916-2927.
- 537 36. Israel EJ, *et al.* (1997) Expression of the neonatal Fc receptor, FcRn, on human
538 intestinal epithelial cells. *Immunology* 92(1):69-74.
- 539 37. Schlachetzki F, Zhu C, & Pardridge WM (2002) Expression of the neonatal Fc receptor
540 (FcRn) at the blood-brain barrier. *J Neurochem* 81(1):203-206.
- 541 38. Zhu X, *et al.* (2001) MHC class I-related neonatal Fc receptor for IgG is functionally
542 expressed in monocytes, intestinal macrophages, and dendritic cells. *J Immunol*
543 166(5):3266-3276.
- 544 39. Pyzik M, *et al.* (2017) Hepatic FcRn regulates albumin homeostasis and susceptibility to
545 liver injury. *Proc Natl Acad Sci U S A* 114(14):E2862-E2871.
- 546 40. Blumberg RS, *et al.* (1995) A major histocompatibility complex class I-related Fc
547 receptor for IgG on rat hepatocytes. *J Clin Invest* 95(5):2397-2402.
- 548 41. Chaudhury C, *et al.* (2003) The major histocompatibility complex-related Fc receptor for
549 IgG (FcRn) binds albumin and prolongs its lifespan. *J Exp Med* 197(3):315-322.
- 550 42. Chaudhury C, Brooks CL, Carter DC, Robinson JM, & Anderson CL (2006) Albumin
551 binding to FcRn: distinct from the FcRn-IgG interaction. *Biochemistry* 45(15):4983-4990.
- 552 43. Good CA, Wells A, & Coyne CB (2018) Type III interferon signaling restricts Enterovirus
553 71 infection of goblet cells. *bioRxiv*.
- 554 44. Leach JL, *et al.* (1996) Isolation from human placenta of the IgG transporter, FcRn, and
555 localization to the syncytiotrophoblast: implications for maternal-fetal antibody transport.
556 *J Immunol* 157(8):3317-3322.
- 557 45. Lozano NA, *et al.* (2018) Expression of FcRn receptor in placental tissue and its
558 relationship with IgG levels in term and preterm newborns. *Am J Reprod Immunol*
559 80(3):e12972.

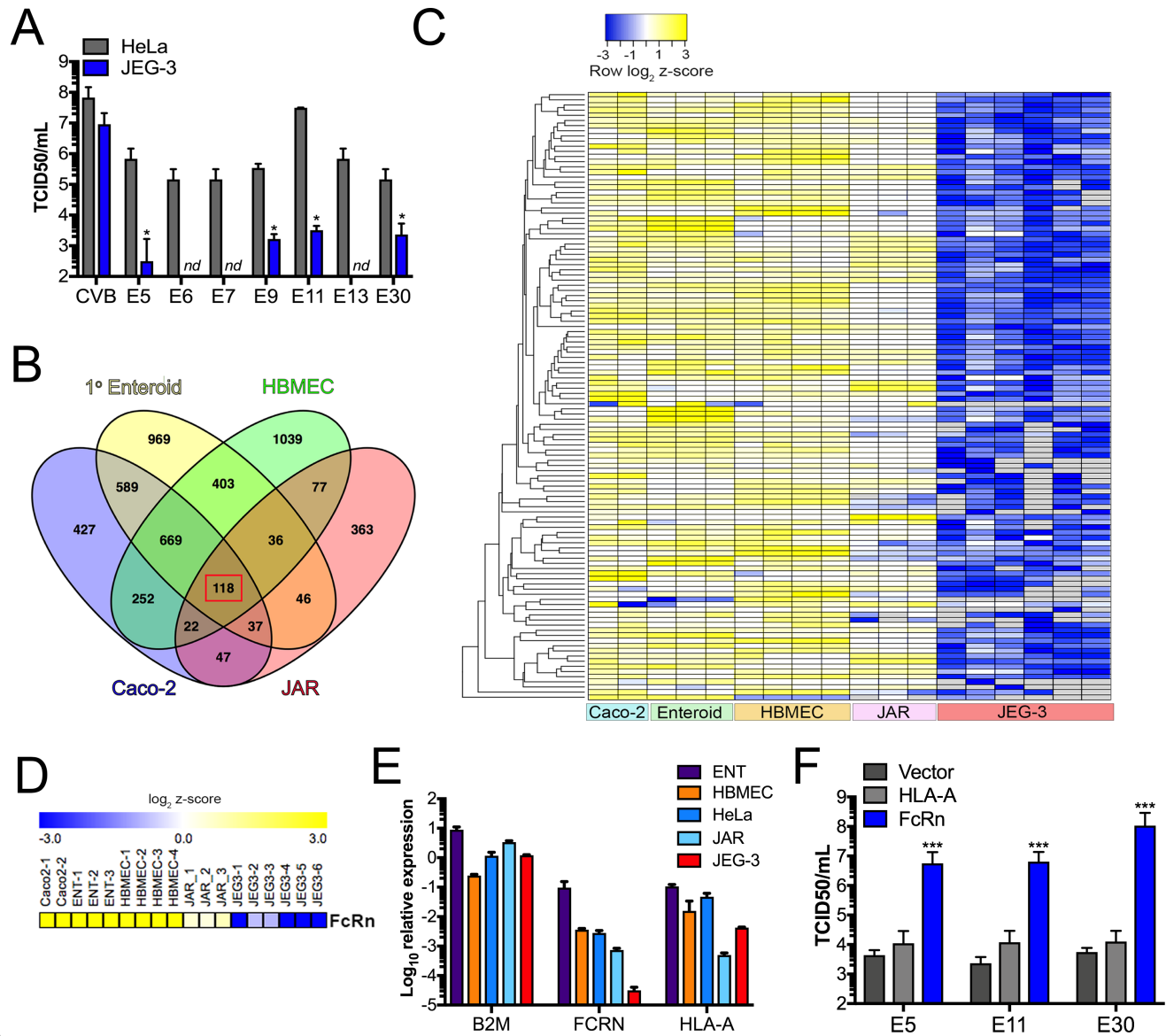
- 560 46. Sockolosky JT & Szoka FC (2015) The neonatal Fc receptor, FcRn, as a target for drug
561 delivery and therapy. *Adv Drug Deliv Rev* 91:109-124.
- 562 47. Stins MF, Badger J, & Sik Kim K (2001) Bacterial invasion and transcytosis in
563 transfected human brain microvascular endothelial cells. *Microb Pathog* 30(1):19-28.
- 564 48. Bayer A, *et al.* (2016) Type III Interferons Produced by Human Placental Trophoblasts
565 Confer Protection against Zika Virus Infection. *Cell Host Microbe* 19(5):705-712.
- 566 49. Drummond CG, Nickerson CA, & Coyne CB (2016) A Three-Dimensional Cell Culture
567 Model To Study Enterovirus Infection of Polarized Intestinal Epithelial Cells. *mSphere*
568 1(1).
- 569 50. Morosky S, Lennemann NJ, & Coyne CB (2016) BPIFB6 Regulates Secretory Pathway
570 Trafficking and Enterovirus Replication. *J Virol* 90(10):5098-5107.
- 571 51. Giannetti AM & Bjorkman PJ (2004) HFE and transferrin directly compete for transferrin
572 receptor in solution and at the cell surface. *J Biol Chem* 279(24):25866-25875.
- 573 52. Savidis G, *et al.* (2016) The IFITMs Inhibit Zika Virus Replication. *Cell Rep* 15(11):2323-
574 2330.
- 575 53. Oberste MS, *et al.* (2006) Species-specific RT-PCR amplification of human
576 enteroviruses: a tool for rapid species identification of uncharacterized enteroviruses. *J*
577 *Gen Virol* 87(Pt 1):119-128.
578

579 **Acknowledgements**

580 We thank Jacqueline Corry and Charles Good (UPMC Children's Hospital of Pittsburgh for
581 technical assistance, Jeffrey Bergelson (Children's Hospital of Philadelphia) for helpful
582 suggestions and reagents, Kwang Sik Kim (Johns Hopkins University) for providing HBMEC, and
583 Terrence Dermody (UPMC Children's Hospital of Pittsburgh) for helpful suggestions. This project
584 was supported by NIH R01-AI081759 (C.B.C.), a Burroughs Wellcome Investigators in the
585 Pathogenesis of Infectious Disease Award (C.B.C), and the Children's Hospital of Pittsburgh of
586 the UPMC Health System (C.B.C). This project also used the UPMC Hillman Cancer Center and
587 Tissue and Research Pathology/Pitt Biospecimen Core and Animal Facility shared resources
588 which are supported in part by award P30CA047904.

589
590
591
592

593 **Figure 1**
594

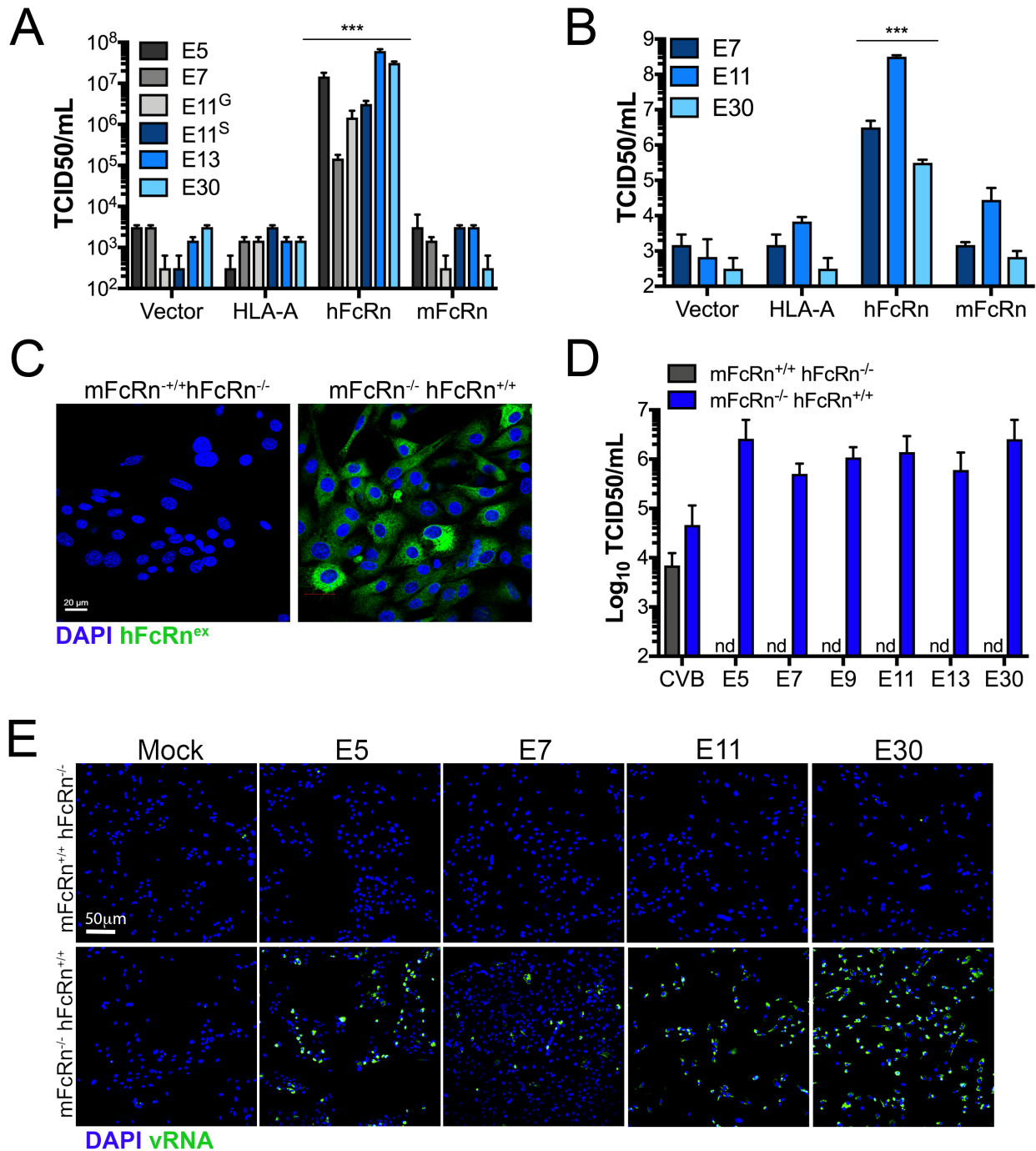


595
596
597 **Figure 1. JEG-3 cells are not infected by echoviruses due to low FcRn expression.** (A),
598 JEG-3 (blue bars) or HeLa (black bars) cells were infected with the indicated echovirus (1
599 PFU/cell) for ~24hrs. Viral titers (log₁₀ TCID50/mL) from the indicated cell types are shown as
600 mean ± standard deviation. Significance was determined using a t-test (p<0.05). (B), Venn
601 diagram from differential expression analysis using the DeSeq2 package in R between JEG-3
602 cells are either primary human fetal-derived enteroids (yellow), HBMEC (green), Caco-2 cells
603 (blue), or JAR cells (red). There were 118 shared genes differentially downregulated between
604 JEG-3 cells and these cell types (red square). (C), Heatmap of 118 genes differentially
605 downregulated in JEG-3 cells and the indicated cell type at bottom) based on log₂ RPKM values.
606 Transcripts with no reads are in grey. (D), Heatmap of FcRn expression in the indicated cell type
607 (based on log₂ RPKM values). (E), RT-qPCR profiling of the level of expression of β2M (B2M),
608 FcRn, or HLA-A in the indicated cell type. Data are shown as log₁₀ relative expression normalized

609 to actin and are shown as mean \pm standard deviation. **(F)**, JEG-3 cells were transfected with
610 vector control (pcDNA) or human HLA-A or FcRn for 24hrs, and then infected with the indicated
611 echovirus for 24hrs. Viral titers (\log_{10} TCID₅₀/mL) are shown as mean \pm standard deviation with
612 significance determined with a Kruskal-Wallis test with Dunn's test for multiple comparisons
613 (**p<0.001). The relative expression of HLA-A and FcRn is shown in Supplemental Figure 1H.

614
615
616
617
618
619
620
621
622
623
624
625
626
627
628
629
630
631
632
633
634
635
636
637
638
639
640
641
642
643
644
645
646
647
648
649
650
651
652
653
654
655

656 **Figure 2**
657

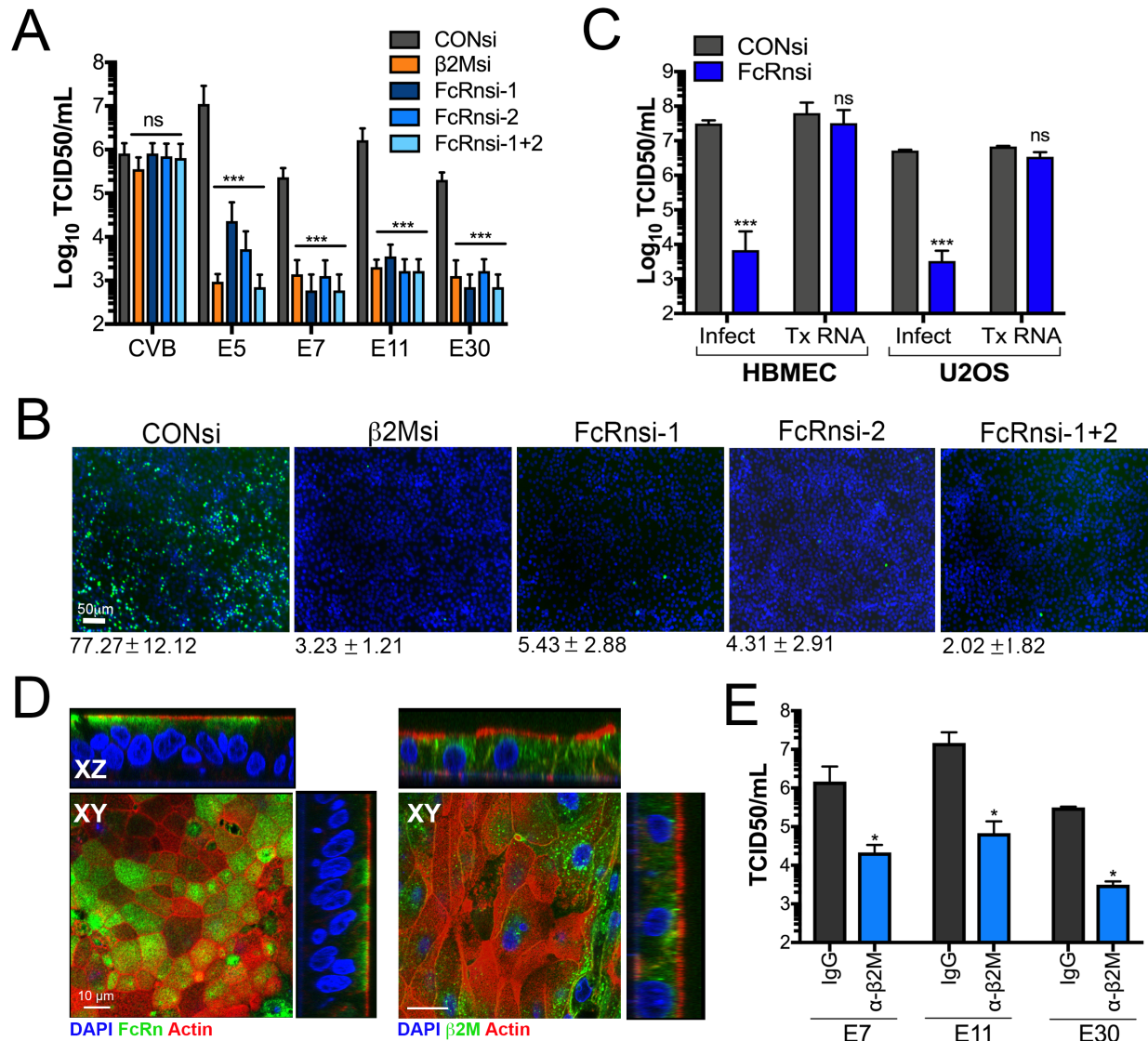


658 **Figure 2. Human, but not mouse, FcRn expression restores infection in human- and**
 659 **mouse-derived cells. (A),** JEG-3 cells were transfected with vector control (pcDNA), human
 660 HLA-A, human FcRn (hFcRn), or mouse FcRn (mFcRn) for 24hrs and then infected with the
 661 indicated echovirus for 24h (E11^G Gregory strain and E11^S Silva strain). Viral titers (log₁₀
 662 TCID50/mL) are shown as mean ± standard deviation with significance determined with a Kruskal-
 663 Wallis test with Dunn's test for multiple comparisons (p<0.001). The relative expression of HLA-
 664
 665

666 A, hFcRn, and mFcRn is shown in Supplemental Figure 2B. **(B)**, Mouse embryonic fibroblasts
667 (MEFs) were transfected with vector control (pcDNA), human HLA-A, or human or mouse FcRn
668 (hFcRn, mFcRn, respectively) for 24hrs and then infected with the indicated echovirus for 24h.
669 Viral titers (\log_{10} TCID50/mL) are shown as mean \pm standard deviation with significance
670 determined with a Kruskal-Wallis test with Dunn's test for multiple comparisons ($p < 0.001$). The
671 relative expression of HLA-A, hFcRn, and mFcRn is shown in Supplemental Figure 2C. **(C)**,
672 Primary fibroblasts were isolated from mice expressing mouse, but not human, FcRn (mFcRn^{+/+}
673 hFcRn^{-/-}) or expressing human, but not mouse, FcRn (mFcRn^{-/-} hFcRn^{+/+}) and then
674 immunostained with an antibody recognizing the extracellular domain of hFcRn (in green). DAPI-
675 stained nuclei are shown in blue. **(D)**, Primary fibroblasts isolated from mFcRn^{+/+} hFcRn^{-/-} mice
676 (grey bars) or mFcRn^{-/-} hFcRn^{+/+} mice (blue bars) were infected with the indicated echovirus, or
677 with coxsackievirus B (CVB) as a control for 24hrs. Viral titers (\log_{10} TCID50/mL) are shown as
678 mean \pm standard deviation from cells isolated from four mice of each type. Nd, not detected. **(E)**,
679 Primary fibroblasts isolated from mFcRn^{+/+} hFcRn^{-/-} or mFcRn^{-/-} hFcRn^{+/+} mice were infected with
680 the indicated echovirus, or mock infected as a control, and then the level of viral replication
681 assessed at 6hrs post-infection by immunofluorescence microscopy for double-stranded viral
682 RNA (a replication intermediate, in green). DAPI-stained nuclei in blue. Scale bars are shown at
683 bottom left in (C) and (E).

684
685
686
687
688
689
690
691
692
693
694
695
696
697
698
699
700
701
702
703
704
705
706
707
708
709
710
711
712
713

714 **Figure 3**
715

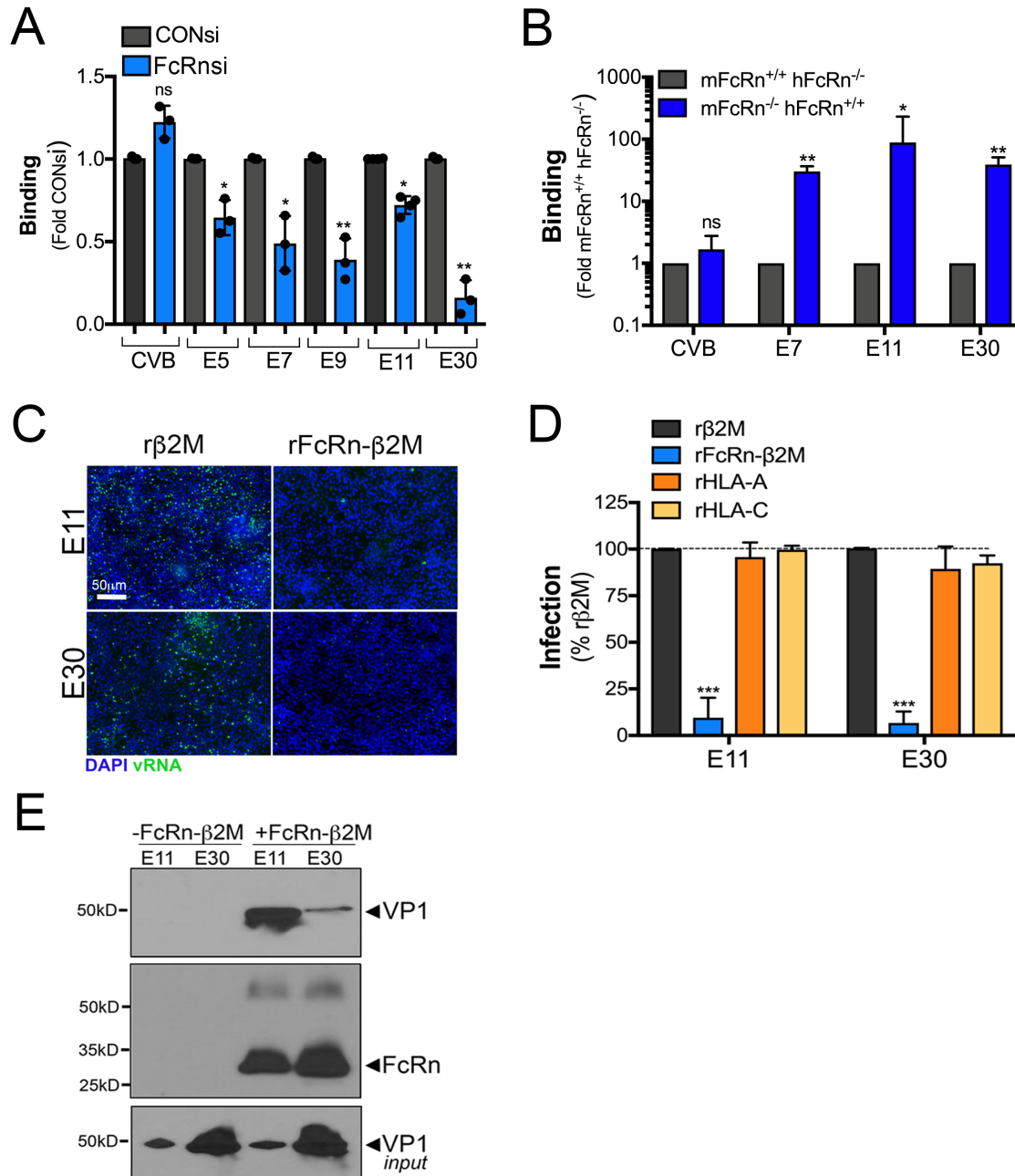


716
717
718 **Figure 3. Loss of FcRn expression reduces echovirus infection.** (A), HBMEC were
719 transfected with an siRNA against β2M (orange bar) or two independent siRNAs against FcRn
720 (FcRn-1 and FcRn-2) alone or in combination (FcRn 1+2) (blue bars), or scrambled control siRNA
721 (CONsi, grey bars) for 48hrs and then infected with CVB or the indicated echovirus for an
722 additional 16hrs. Shown are viral titers (log₁₀ TCID₅₀/mL) as mean ± standard deviation with
723 significance determined with a Kruskal-Wallis test with Dunn's test for multiple comparisons
724 (**p<0.001, ns not significant). (B), HBMEC transfected with siRNAs as described in (A) were
725 infected with E11 for 24hrs and then infection assessed by immunofluorescence microscopy for
726 double stranded viral RNA (a replication intermediate, in green). DAPI-stained nuclei are shown
727 in blue. The average level of infection (as determined by the percent of DAPI-stained nuclei that
728 were positive for vRNA) is shown at bottom as mean ± standard deviation. (C), HBMEC
729 transfected with scrambled control siRNA (CONsi) or FcRn siRNA (FcRnsi-1) for 48hrs were
730 infected with E11 or transfected with infectious E11 viral RNA for an additional 24hrs. Shown are

731 viral titers (\log_{10} TCID₅₀/mL) as mean \pm standard deviation with significance determined with a t-
732 test (**p<0.001, ns not significant). **(D)**, Confocal micrographs of fetal-derived primary human
733 intestinal epithelial (HIE) cells immunostained for FcRn (left, green) or b2M (right, green) and
734 counterstained for actin (left and right, red). DAPI-stained nuclei are shown in blue. Three-
735 dimensional cross-sections are shown at top and right. Scale bars at bottom left. **(E)**, Primary fetal
736 HIE were incubated with anti- β 2M monoclonal antibody (blue bars) or isotype control antibody
737 (grey bars) (2 μ g/mL for both) for 30min prior to infection with the indicated echovirus in the
738 presence of antibody for an additional 24hrs. Shown are viral titers (\log_{10} TCID₅₀/mL) as mean
739 \pm standard deviation from three independent HIE preparations with significance determined with
740 a t-test (*p<0.05).

741
742
743
744
745
746
747
748
749
750
751
752
753
754
755
756
757
758
759
760
761
762
763
764
765
766
767
768
769
770
771
772
773
774
775
776
777

778 **Figure 4**
779



780 **Figure 4. FcRn mediates echovirus binding.** (A), HBMEC were transfected with an siRNA
781 against FcRn (FcRn-1, blue bars) or scrambled control siRNA (CONsi, grey bars) for 48hrs and
782 then the extent of viral binding of CVB or the indicated echovirus (50 PFU/cell) as assessed by a
783 RT-qPCR based binding assay. The extent of binding is shown as a fold from CONsi control
784 (mean ± standard deviation). Significance was determined using a t-test (*p<0.05, ns not
785 significant). (B), The extent of viral binding of CVB or the indicated echovirus (50 PFU/cell) was
786 assessed in primary fibroblasts isolated from mFcRn^{+/+} hFcRn^{-/-} or mFcRn^{-/-} hFcRn^{+/+} mice using
787 a RT-qPCR based binding assay. Shown is the extent of binding in cells isolated from four mice
788

789 of each type, which is shown as mean \pm standard deviation. Significance was determined using
790 a t-test (* $p < 0.05$, ** $p < 0.01$, ns not significant). **(C)**, E11 or E30 (10^6 particles) were incubated with
791 recombinant $\beta 2M$ (r $\beta 2M$, 2.5 $\mu g/mL$) or the extracellular domain of FcRn in complex with $\beta 2M$
792 (rFcRn- $\beta 2M$, 2.5 $\mu g/mL$) for 1hr at 4°C, pre-adsorbed to HBMEC for 1hr at 4°C, washed, and then
793 cells infected for 16hrs. Shown are representative immunofluorescence images for double
794 stranded viral RNA (a replication intermediate, green). DAPI-stained nuclei are shown in blue.
795 **(D)**, E11 or E30 (10^6 particles) were incubated with recombinant $\beta 2M$ (r $\beta 2M$, 2.5 $\mu g/mL$), FcRn in
796 complex with $\beta 2M$ (rFcRn- $\beta 2M$, 2.5 $\mu g/mL$), HLA-A (2.5 $\mu g/mL$), or HLA-C (2.5 $\mu g/mL$) for 1hr at
797 4°C, pre-adsorbed to HBMEC for 1hr at 4°C, washed, and then cells infected for 16hrs. The level
798 of infection was assessed by immunostaining for vRNA normalized to DAPI-stained nuclei. Shown
799 is the perfect of infection normalized to r $\beta 2M$ controls from experiments performed in triplicate
800 (>1000 cells total) as mean \pm standard deviation. Significance was determined with a Kruskal-
801 Wallis test with Dunn's test for multiple comparisons (** $p < 0.001$). **(E)**, E11 or E30 (10^8 particles)
802 were incubated with recombinant $\beta 2M$ (r $\beta 2M$, 5 $\mu g/mL$) or 6x His-tagged extracellular domain of
803 FcRn in complex with $\beta 2M$ (rFcRn- $\beta 2M$, 5 $\mu g/mL$) for 1hr at 4°C, then incubated with Ni-NTA
804 Agarose beads for 1hr at 4°C. Following extensive washing, immunoblots were performed for the
805 viral capsid protein VP1 (top) and then membranes were stripped and re-probed with an antibody
806 recognizing the extracellular domain of FcRn (middle). In parallel, level of input virus was
807 immunoblotted with anti-VP1 antibody (bottom).

808
809
810
811
812
813
814
815
816
817
818
819
820
821
822
823
824
825
826
827
828
829
830
831
832
833
834
835
836